

IMPROVING HERITABILITY ESTIMATION BY A VARIABLE SELECTION APPROACH IN SPARSE HIGH DIMENSIONAL LINEAR MIXED MODELS

A. BONNET, C. LÉVY-LEDUC, E. GASSIAT, R. TORO, AND T. BOURGERON

ABSTRACT. Motivated by applications in neuroanatomy, we propose a novel methodology for estimating the heritability which corresponds to the proportion of phenotypic variance which can be explained by genetic factors. Estimating this quantity for neuroanatomical features is a fundamental challenge in psychiatric disease research. Since the phenotypic variations may only be due to a small fraction of the available genetic information, we propose an estimator of the heritability that can be used in high dimensional sparse linear mixed models. Our method consists of three steps. Firstly, a variable selection stage is performed in order to recover the support of the genetic effects – also called causal variants – that is to find the genetic effects which really explain the phenotypic variations. Secondly, we propose a maximum likelihood strategy for estimating the heritability which only takes into account the causal genetic effects found in the first step. Thirdly, we compute the standard error and the 95% confidence interval associated to our heritability estimator thanks to a nonparametric bootstrap approach. Our contribution consists in providing an estimation of the heritability with standard errors substantially smaller than methods without variable selection when the genetic effects are very sparse. Since the real genetic architecture is in general unknown in practice, we also propose an empirical criterion which allows the user to decide whether it is relevant to apply a variable selection based approach or not. We illustrate the performance of our methodology on synthetic and real neuroanatomic data coming from the Imagen project. We also show that our approach has a very low computational burden and is very efficient from a statistical point of view.

1. INTRODUCTION

For many complex traits in human population, there exists a huge gap between the genetic variance explained by population studies and the variance explained by specific variants found thanks to genome wide association studies (GWAS). This gap has been called by [9] and [10] the “dark matter” of the genome or the “dark matter” of heritability. Various

population studies have shown that up to 80% of the variability of neuroanatomical phenotypes such as the brain volume could be explained by genetic factors, see for instance [17]. This result is very important since several psychiatric disorders are shown to be associated to neuroanatomical changes, for instance macrocephaly and autism [16] or blackuced hippocampus and schizophrenia [1]. Estimating properly the impact of the genetic background on neuroanatomical changes is a crucial challenge in order to determine afterwards if this background can either be a risk factor or a protective factor from developing psychiatric disorders. The GWAS studies performed for instance by [17] identified genetic variants involved in the neuroanatomical diversity, which contributes to understand the impact of genetic factors. However, in the course of these studies, it is shown that this approach only explains a small proportion of the phenotypic variance. In order to understand the nature of the genetic factors responsible for major variations of the brain volume, [19] used linear mixed models (LMM) to consider the effects of all the common genetic diversity characterized by the Single Nucleotide Polymorphisms (SNPs). This approach had been suggested by [22] to study the effects of the SNPs on the height variations. The model they consider is a LMM defined as follows:

$$(1) \quad \mathbf{Y} = \mathbf{X}\boldsymbol{\beta} + \mathbf{Z}\mathbf{u} + \mathbf{e} ,$$

where $\mathbf{Y} = (Y_1, \dots, Y_n)'$ is the vector of observations (phenotypes), \mathbf{X} is a $n \times p$ matrix of predictors, $\boldsymbol{\beta}$ is a $p \times 1$ vector containing the unknown linear effects of the predictors, \mathbf{Z} is the genetic information matrix, \mathbf{u} and \mathbf{e} correspond to the random effects. More precisely, \mathbf{Z} is a version of \mathbf{W} with centered and normalized columns, where \mathbf{W} is defined as follows: $W_{i,j} = 0$ (resp. 1, resp. 2) if the genotype of the i th individual at locus j is qq (resp. Qq , resp. QQ) where p_j denotes the frequency of the allele q at locus j . In (1), the vector \mathbf{e} corresponds to the environment effects and the vector \mathbf{u} corresponds to the genetic random effect, that is the j -th component of u is the effect of the j -th SNP on the phenotype. In the modeling of [22], all the SNPs have an effect on the considered phenotype, that is

$$(2) \quad \mathbf{u} \sim \mathcal{N}\left(0, \sigma_u^2 \text{Id}_{\mathbb{R}^n}\right) \text{ and } \mathbf{e} \sim \mathcal{N}\left(0, \sigma_e^2 \text{Id}_{\mathbb{R}^n}\right) .$$

The covariance matrix of \mathbf{Y} can thus be written as:

$$\text{Var}(\mathbf{Y}) = N\sigma_u^2 \mathbf{R} + \sigma_e^2 \text{Id}_{\mathbb{R}^n} , \text{ where } \mathbf{R} = \frac{\mathbf{Z}\mathbf{Z}'}{N} ,$$

and the parameter η^* defined as

$$(3) \quad \eta^* = \frac{N\sigma_u^{*2}}{N\sigma_u^{*2} + \sigma_e^{*2}}$$

is commonly called the heritability ([22],[14]), and corresponds to the proportion of phenotypic variance which is determined by all the SNPs.

Since all SNPs are not necessarily causal, it seems more realistic to extend the previous modeling by assuming that the genetic random effects can be sparse, that is only a proportion q of the components of \mathbf{u} are non null:

$$(4) \quad u_i \stackrel{i.i.d.}{\sim} (1 - q)\delta_0 + q\mathcal{N}(0, \sigma_u^{*2}), \text{ for all } 1 \leq i \leq N,$$

where q is in $(0, 1]$, and δ_0 is the point mass at 0. Then the definition of η^* has to be adjusted as follows:

$$(5) \quad \eta^* = \frac{Nq\sigma_u^{*2}}{Nq\sigma_u^{*2} + \sigma_e^{*2}}.$$

It corresponds to the proportion of phenotypic variance which is due to a certain number of causal SNPs which are, obviously, unknown. Let us emphasize that, in most applications, the proportion q of causal SNPs is also unknown, and that it may happen that the scientist has no idea how small q is.

When $q = 1$, that is when considering the modeling (2), most proposed approaches to estimate the heritability derive from a likelihood methodology. We can quote for instance the REstricted Maximum Likelihood (REML) strategies, originally proposed by [13] and then developed in [15]. Several approximations of the REML algorithm have also been proposed, see for instance the software EMMA proposed by [14] or the software GCTA ([22],[21]).

We proposed in [4] another method based on a maximum likelihood strategy to estimate the heritability and implemented in the R package HiLMM. We proved in [4] the following theoretical result: though the computation of the likelihood is based on the modeling assumption (2), the estimator is consistent (unbiased) under the less restrictive modeling assumption (4). We believe this consistency result remains true for the estimators produced using the algorithms REML, EMMA, GCTA. But we also proved that, when $q \neq 1$, the standard error is not the one computed by the softwares when $q = 1$ and may be very large. We obtained a theoretical formula for the asymptotic variance of the estimator (depending in particular on q) and conducted several numerical experiments to understand how this asymptotic variance

gets larger depending on the various quantities, in particular with respect to q and the ratio n/N . We observed that this variance indeed gets larger when q gets smaller, so that the accuracy of the heritability estimator is slightly deteriorated when all SNPs are not causal. Thus, a first problem is to find a method able to produce an estimator with smaller standard error than those obtained using only likelihood strategies. Also, since this standard error depends on q , a second problem is to produce a confidence interval one could trust without knowing q .

The goal of this paper is to address both problems. The results we obtained in [4] suggest the following. If we knew the set of causal SNPs, then, considering only this (small) subset in the genetic information matrix, we would obtain with HiLMM an estimator having a smaller standard error than when using all SNPs in the genetic information matrix. Thus, our new practical method contains a variable selection step.

Variable selection and signal detection in high dimensional linear models have been extensively studied in the past decade and there are many papers on this subject. Among them, we can quote [11] and [2] about variable selection and references therein. The case of high dimensional mixed models has received little attention. As far as variable selection methods in the random effects of LMM are concerned, we are only aware of the work of [6] and [3]. Let us mention that regarding the estimation of heritability with possible sparse effects, there is also the bayesian approach of [7] and [23], which proposes an interesting estimator for the heritability but which is computationally very demanding. Notice that, in our framework, we are not far from the situation for which it is proved in [20] that the support cannot be fully recovered, which happens when $Nq \log(1/q) \gg n$. The variable selection step we propose takes elements from both ultrahigh dimension methods ([5], [8], [11]) and classical variable selection techniques ([18]).

The second step of our method is to apply HiLMM using the selected subset of causal SNPs produced by the first step. Finally, we propose a non parametric bootstrap procedure to get confidence intervals with prescribed coverage. The whole procedure requires only a few minutes of computation.

To conclude, we propose in this paper a very fast method to estimate the heritability and construct a confidence interval substantially smaller than without variable selection when the genetic effects are very sparse. Since the real genetic architecture is in general unknown in

practice, we also propose an empirical criterion which allows the user to decide whether it is relevant to apply a variable selection based approach or not. Our method has also the advantage to return a list of SNPs possibly involved in the variations of a given quantitative feature. This set of SNPs can further be analyzed from a biological point of view.

The paper is organized as follows. Section 2 describes the data set which motivated our work. Section 3 provides the detailed description of the method, and Section 4 displays the results of the numerical study. They were obtained by using the R package EstHer that we developed and which is available from the Comprehensive R Archive Network (CRAN). The simulation results illustrate the performance of our method on simulations and show that it is very efficient from a statistical point of view. In Section 5, we provide an empirical criterion to help the user to decide whether it is relevant to apply a variable selection based approach or not. In Section 6, we propose a thorough comparison of our approach with other methods in terms of statistical and numerical performances. Finally, the results obtained on the brain data described in Section 2 can be found in Section 7. We also provide a discussion section at the end of the paper.

2. DESCRIPTION OF THE DATA

We worked on data sets provided by the European project Imagen, which is a major study on mental health and risk taking behaviour in teenagers. The research program includes questionnaires, interviews, behaviour tests, neuroimaging of the brain and genetic analyses. We will focus here on the genetic information collected on approximately 2000 teenagers as well as measurements of the volume of several features: the intracranial brain volume (icv), the thalamus (th), the caudate nucleus (ca), the amygdala (amy), the globus pallidus (pa), the putamen (pu), the hippocampus (hip), the nucleus accubens (acc) and the total brain volume (bv). Figure 1, which comes from [19], is a schematic representation of these different areas of the brain. The data set contains $n = 2087$ individuals and $N = 273926$ SNPs, as well as a set of fixed effects, which in our case are the age (between 12 and 17), the gender and the city of residency (London, Nottingham, Dublin, Dresden, Berlin, Hamburg, Mannheim and Paris).

In the following, our goal will thus be to provide a method to estimate the heritability of these neuroanatomical features.

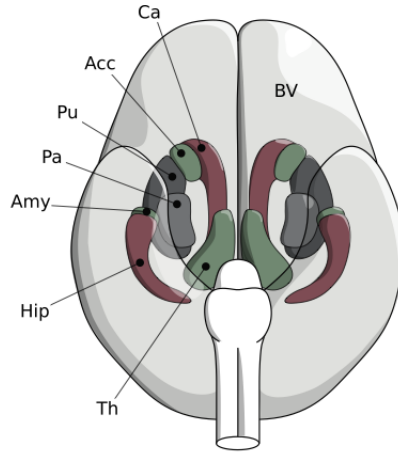


FIGURE 1. Different regions of the brain (this figure is taken from [19]).

3. DESCRIPTION OF THE METHOD

The method that we propose can be split into two main parts: the first one consists in a variable selection approach and the second one provides an estimation of the heritability and the associated 95% confidence interval which is computed by using non parametric bootstrap.

At the beginning of this section we shall consider the case where there is no fixed effects, that is

$$(6) \quad \mathbf{Y} = \mathbf{Z}\mathbf{u} + \mathbf{e}$$

but we explain at the end of this section how to deal with fixed effects. Let us first describe our variable selection method which consists of three steps.

3.1. Variable selection. Inspired by the ideas of [5], we do not directly apply a Lasso type approach since we are in an ultra-high dimension framework. Hence, we start our variable selection stage by the SIS (Sure Independence Screening) approach, as suggested by [5], in order to select the components of \mathbf{u} which are the most correlated to the response \mathbf{Y} and then we apply a Lasso criterion which depends on a regularization parameter λ . This regularization parameter is usually chosen by cross validation but here we decided to use the stability selection approach devised by [11] which provided better results in our framework.

Step 1: Empirical correlation computation. The first step consists in blackucing the number of relevant columns of \mathbf{Z} by trying to remove those associated to null components in the vector \mathbf{u} . For this, we use the SIS (Sure Independence Screening) approach proposed by [5] and improved by [8] in the ultra-high dimensional framework. More precisely, we compute for each column j of \mathbf{Z} :

$$C_j = \left| \sum Y_i Z_{i,j} \right|,$$

and we only keep the N_{\max} columns of \mathbf{Z} having the largest C_j . In practice, we choose the conservative value $N_{\max} = n$, inspiblack by the comments of [5] on the choice of N_{\max} .

In the sequel, we denote by $\mathbf{Z}_{\text{black}}$ the matrix containing these n relevant columns. This first step is essential for our method. Indeed, on the one hand, it substantially decreases the computational burden of our approach and on the other hand, it blackuces the size of the data and thus makes classical variable selection tools efficient.

Step 2: LASSO criterion and stability selection. In order to refine the set of columns (or components of \mathbf{u}) selected in the first step and to remove the remaining null components in the vector \mathbf{u} , we apply a Lasso criterion originally devised by [18] which has been used in many different contexts and has been thouroughly theoretically studied. It consists in minimizing with respect to u the following criterion:

$$(7) \quad \text{Crit}_\lambda(u) = \|\mathbf{Y} - \mathbf{Z}_{\text{black}}u\|_2^2 + \lambda\|u\|_1,$$

which depends on the parameter λ and where $\|x\|_2^2 = \sum_{i=1}^p x_i^2$ and $\|x\|_1 = \sum_{i=1}^p |x_i|$ for $x = (x_1, \dots, x_p)$. The choice of the regularization parameter λ is crucial since its value may strongly affect the selected variables set. Different approaches have been proposed for choosing this parameter such as cross-validation which is implemented for instance in the `glmnet` R package. Here we shall use the following strategy based on the stability selection proposed by [11].

The vector of observations \mathbf{Y} is randomly split into several subsamples of size $n/2$. For each subsample, we apply the LASSO criterion for a fixed parameter λ and the selected variables are stoblack. Then, for a given threshold, we keep in the final set of selected variables only the variables appearing a number of times larger than this threshold. In practice, we generated 50 subsamples of \mathbf{Y} and we chose the parameter λ as the smallest value of the regularization path. As explained in [12], such a choice of λ ensures that some overfitting occurs and hence

that the set of selected variables is large enough to include the true variables with high probability.

The matrix \mathbf{Z} containing only the final set of selected columns will be denoted by $\mathbf{Z}_{\text{final}}$ in the following, where N_{final} denotes its number of columns.

The threshold has to be chosen carefully: keeping too many columns in $\mathbf{Z}_{\text{final}}$ could indeed lead to overestimating the heritability and, on the contrary, removing too many columns of \mathbf{Z} could lead to underestimating the heritability. In the “small q ” situations where it is relevant to use a variable selection approach a range of thresholds in which the heritability estimation is stable will appear as suggested by [12]. In practice, we simulate observations \mathbf{Y} satisfying (6), by using the matrix \mathbf{Z} , for different values of q and for different values η^* and we observe that this stability region for the threshold appear for small values of q . This procedure is further illustrated in Section 4.

3.2. Heritability estimation and confidence interval.

3.2.1. *Heritability estimation.* For estimating the heritability, we used the approach that we proposed in [4]. It is based on a maximum likelihood strategy and was implemented in the R package HiLMM. Let us recall how this method works.

In the case where $q = 1$, which corresponds to the non sparse case,

$$\mathbf{Y} \sim \mathcal{N}\left(0, \eta^* \sigma^{*2} \mathbf{R} + (1 - \eta^*) \sigma^{*2} \text{Id}_{\mathbb{R}^n}\right),$$

with $\sigma^{*2} = N\sigma_u^{*2} + \sigma_e^{*2}$ and $\mathbf{R} = \mathbf{Z}_{\text{final}} \mathbf{Z}'_{\text{final}} / N_{\text{final}}$, where $\mathbf{Z}_{\text{final}}$ denotes the matrix \mathbf{Z} in which the columns selected in the variable selection step described in Section 3.1 are kept.

Let \mathbf{U} be defined as follows: $\mathbf{U}'\mathbf{U} = \mathbf{U}\mathbf{U}' = \text{Id}_{\mathbb{R}^n}$ and $\mathbf{U}\mathbf{R}\mathbf{U}' = \text{diag}(\lambda_1, \dots, \lambda_n)$, where the last quantity denotes the diagonal matrix having its diagonal entries equal to $\lambda_1, \dots, \lambda_n$. Hence, in the case where $q = 1$,

$$(8) \quad \tilde{\mathbf{Y}} = \mathbf{U}'\mathbf{Y} \sim \mathcal{N}(0, \Gamma)$$

$$\text{with } \Gamma = \text{diag}(\eta^* \sigma^{*2} \lambda_1 + (1 - \eta^*) \sigma^{*2}, \dots, \eta^* \sigma^{*2} \lambda_n + (1 - \eta^*) \sigma^{*2}),$$

where the λ_i 's are the eigenvalues of \mathbf{R} .

We propose to define $\hat{\eta}$ as a maximizer of the log-likelihood

$$(9) \quad L_n(\eta) = -\log\left(\frac{1}{n} \sum_{i=1}^n \frac{\tilde{Y}_i^2}{\eta(\lambda_i - 1) + 1}\right) - \frac{1}{n} \sum_{i=1}^n \log(\eta(\lambda_i - 1) + 1),$$

where the \tilde{Y}_i 's are the components of the vector $\tilde{\mathbf{Y}} = \mathbf{U}'\mathbf{Y}$.

We now explain how to obtain accurate confidence intervals for the heritability by using a non parametric bootstrap approach.

3.2.2. *Bootstrap confidence interval.* We used the following procedure:

- Step 1: We estimate η^* and σ^{*2} by using our approach described in the previous subsection. The corresponding estimators are denoted $\hat{\eta}$ and $\hat{\sigma}$.
- Step 2: We compute $\mathbf{Y}_{\text{new}} = \hat{\Gamma}^{-1/2}\tilde{\mathbf{Y}}$, where $\tilde{\mathbf{Y}}$ is defined in (8) and $\hat{\Gamma}$ has the same structure as Γ defined in (8) except that η^* and σ^* are replaced by their estimators $\hat{\eta}$ and $\hat{\sigma}$, respectively.
- Step 3: We create K vectors $(\mathbf{Y}_{\text{new},i})_{1 \leq i \leq K}$ from \mathbf{Y}_{new} by randomly choosing each of its components among those of \mathbf{Y}_{new} .
- Step 4: We then build K new vectors $(\tilde{\mathbf{Y}}_{\text{samp},i})_{1 \leq i \leq K}$ as follows: $\tilde{\mathbf{Y}}_{\text{samp},i} = \hat{\Gamma}\mathbf{Y}_{\text{new},i}$. For each of them we estimate the heritability. We thus obtain a vector of heritability estimators $(\hat{\eta}_1, \dots, \hat{\eta}_K)$.
- Step 5: For obtaining a 95% bootstrap confidence interval, we order these values of $\hat{\eta}_k$ and keep the ones corresponding to the $[0.975 \times K]$ largest and the $[0.025 \times K]$ smallest, where $[x]$ denotes the integer part of x . These values define the upper and lower bounds of the 95% bootstrap confidence interval for the heritability η^* , respectively.

A bootstrap estimator of the variance can be obtained by computing the empirical variance estimator of the $\hat{\eta}_k$'s. In practice, we chose $K = 80$ replications.

In Step 2 of the previous algorithm, we should be in the non sparse case $q = 1$ thanks to the variable selection stage. Hence, the covariance matrix of \mathbf{Y}_{new} should be close to identity.

Observe that our resampling technique is close to the one proposed by [?] for building permutation tests in linear mixed models.

3.3. Additional fixed effects. The method described above does not take into account the presence of fixed effects. For dealing with such effects we propose to use the following method, which mainly consists in projecting the observations onto the orthogonal of $\text{Im}(\mathbf{X})$, the image of \mathbf{X} , to get rid of the fixed effects. In practice, instead of considering \mathbf{Y} and \mathbf{Z} we consider

$\tilde{\mathbf{Y}} = \mathbf{A}'\mathbf{Y}$ and $\tilde{\mathbf{Z}} = \mathbf{A}'\mathbf{Z}$, where \mathbf{A} is a $n \times (n - d)$ matrix (d being the rank of the fixed effects matrix), such that $\mathbf{A}\mathbf{A}' = \mathbf{P}_{\mathbf{X}}$, $\mathbf{A}'\mathbf{A} = \text{Id}_{\mathbb{R}^{n-d}}$ and $\mathbf{P}_{\mathbf{X}} = \text{Id}_{\mathbb{R}^n} - \mathbf{X}(\mathbf{X}'\mathbf{X})^{-1}\mathbf{X}'$. This procedure was for instance used by [6].

4. NUMERICAL STUDY

We present in this section the numerical results obtained with our approach which is implemented in the R package EstHer.

4.1. Simulation process. Since in genetic applications, the number n of individuals is very small with respect to the number N of SNPs, we chose $n = 2000$ and $N = 100000$ in our numerical study. We also set $\sigma_u^{*2} = 1$, we shall consider different values for q and we shall change the value of σ_e^* in order to have the following values for η^* : 0.4, 0.5, 0.6 and 0.7. We generate a matrix \mathbf{W} such that its columns W_j are independent binomial random variables of parameters n and p_j , where p_j is randomly chosen in $[0.1, 0.5]$. We compute \mathbf{Z} by centering and empirically normalizing the matrix \mathbf{W} . The random effects are generated according to Equation (4) and then we compute a vector of observations such that $\mathbf{Y} = \mathbf{Z}\mathbf{u} + \mathbf{e}$.

We can make two important comments about the previous simulation process. Firstly, we generated a matrix \mathbf{W} with independent columns, that is we assume that the SNPs are not correlated. Since this assumption may not be very realistic in practice, we provide in Section 4.2.5 some additional simulations where the generated matrix \mathbf{W} has been replaced by the real matrix \mathbf{W} coming from the IMAGEN project. Secondly, we did not include fixed effects but we show some results in Section 4.2.4 when fixed effects are taken into account.

4.2. Results in very sparse scenarios. In this section, we shall focus on the performances of our method in a very sparse scenario, that is 100 causal SNPs out of 100,000. We will describe all the results in terms of heritability estimation, support recovery and computational times in this particular case, then we will study other sparsity scenarios.

4.2.1. Choice of the threshold. In order to determine the threshold, we apply the procedure described in Section 3.1 and 3.2.1. Figure 2 displays the mean of the absolute value of the difference between η^* and the estimated value $\hat{\eta}$ for different thresholds and for different values of η^* obtained from 10 replications. We can see from this figure that in the case where the number of causal SNPs is relatively small: 100, that is $q = 10^{-3}$, our estimation

procedure provides relevant estimations of the heritability for a range of thresholds around 0.75. Moreover, the optimal threshold leading to the smallest gap between $\hat{\eta}$ for different values of η^* is 0.76. We will use this value in the following numerical study. However, the way of choosing the threshold will be further discussed, especially in the section dedicated to the study of the genetic data.

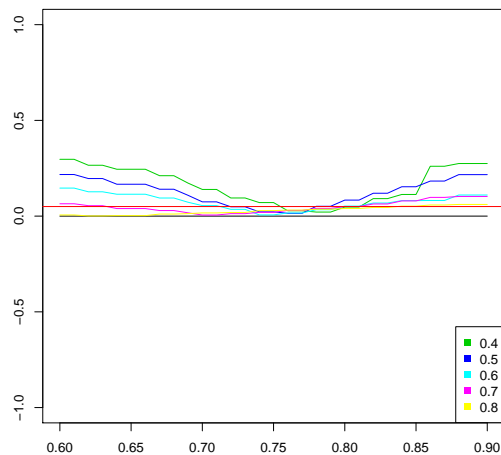


FIGURE 2. Absolute difference between η^* and $\hat{\eta}$ for thresholds from 0.6 to 0.9 and for $q = 10^{-3}$ (100 causal SNPs).

4.2.2. *Confidence intervals.* We use the non parametric bootstrap approach described in Section 3 in order to compute the confidence intervals associated to the estimations of the heritability. Table 1 shows that the 95% confidence intervals obtained by bootstrap and the empirical confidence intervals are very similar. The empirical confidence intervals are computed as follows: the different estimations of η^* obtained along the different replications are ordered, the $[0.975 \times M]$ largest and the $[0.025 \times M]$ smallest values correspond to the upper (resp. lower) bound of the 95% empirical confidence interval. Here, $[x]$ denotes the integer part of x and M is the number of replications. From Table 1, we can see that the empirical confidence intervals are included in the bootstrap intervals, which means that our approach provides conservative intervals.

4.2.3. *Comparison between the methods with and without selection.* Our results are comparable to those obtained if we do not perform the selection before the estimation, that is with the method implemented in HiLMM ("without"), but also with an approach which

TABLE 1. 95 % confidence intervals for $\hat{\eta}$ obtained empirically and by our Bootstrap method.

η^*	0.4	0.5	0.6	0.7
Bootstrap	[0.353 ; 0.503]	[0.413 ; 0.565]	[0.494 ; 0.654]	[0.596 ; 0.738]
Empirical	[0.391 ; 0.470]	[0.449 ; 0.542]	[0.496 ; 0.645]	[0.618 ; 0.720]

TABLE 2. 95 % confidence intervals for $\hat{\eta}$ obtained by our approach, GCTA, the oracle approach and the approach without selection (“without”).

η^*	0.4	0.5	0.6	0.7
EstHer	[0.353 ; 0.503]	[0.413 ; 0.565]	[0.494 ; 0.654]	[0.596 ; 0.738]
Oracle	[0.362 ; 0.472]	[0.414 ; 0.563]	[0.529 ; 0.670]	[0.619 ; 0.745]
without	[0.120 ; 0.880]	[0.102 ; 0.812]	[0.320 ; 0.938]	[0.349 ; 0.932]

assumes the position of the non null components to be known (oracle). The results are displayed in Figure 3 and in Table 3. In this table, the confidence intervals displayed for the lines “Oracle” and “without” are obtained by using the asymptotic variance derived in [4] which corresponds to the classical inverse of the Fisher information in the case $q = 1$. We observe that our method without the selection step provides similar results, that is almost no bias but a very large variance due to the framework $N \gg n$. Our method EstHer considerably blackuces the variance compablack to this method and exhibits performances close to those of the oracle approach which, contrary to our approach, knows the position of the non null components.

4.2.4. *Additional fixed effects.* We generated some synthetic data according to the process described in Section 4.1 but we added a matrix of fixed effects containing two colums. Figure 4 (a) displays the corresponding results which show that the presence of fixed effects does not alter the heritability estimation.

4.2.5. *Simulations with the matrix \mathbf{W} of the IMAGEN data set.* We conducted some additional simulations in order to see the impact of the linkage disequilibrium, that is the possible correlations between the columns of \mathbf{Z} . Indeed, in the previous numerical study, we generated a matrix \mathbf{W} with independent columns. The matrix \mathbf{W} that we use now to generate the

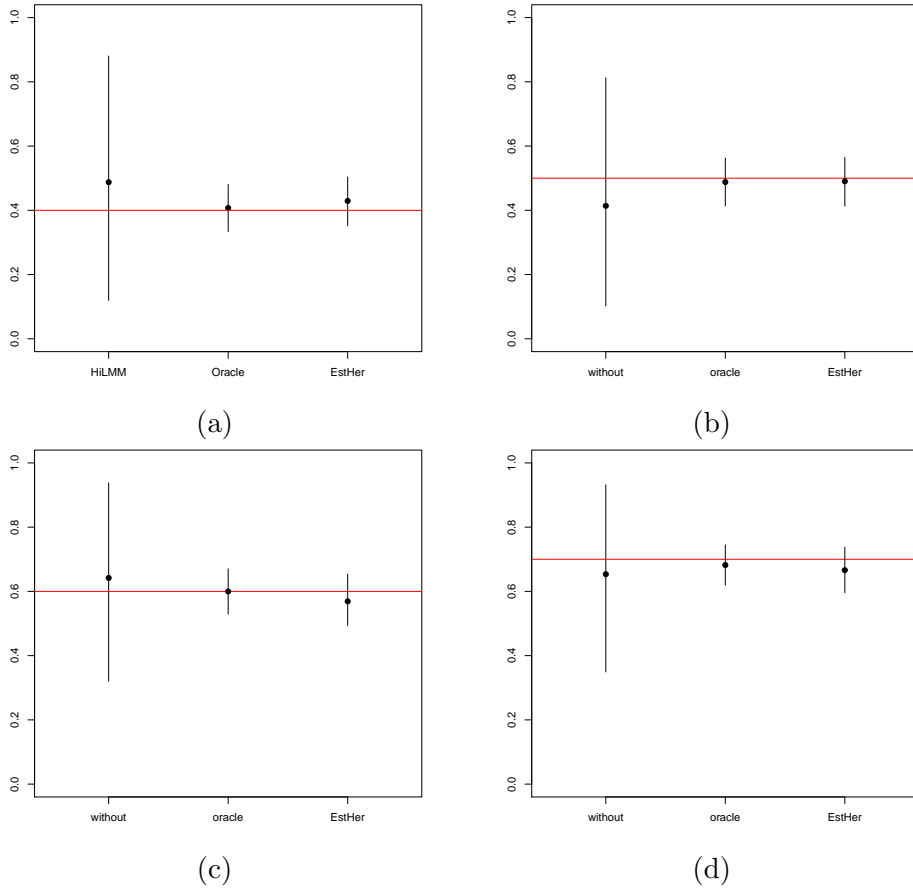


FIGURE 3. Estimation of the heritability and the corresponding 95% confidence intervals when $q = 10^{-3}$, and for different values of η^* : (a) $\eta^* = 0.4$, (b) $\eta^* = 0.5$, (c) $\eta^* = 0.6$, (d) $\eta^* = 0.7$. The means of the heritability estimators (displayed with black dots), the means of the lower and upper bounds of the 95% confidence intervals are obtained from 20 replicated data sets for the different methods: without selection (“without”), “oracle” which knows the position of the null components and EstHer. The horizontal gray line corresponds to the value of η^* .

observations is the one from our genetic data set, except that we truncated it in order to have $n = 2000$ and $N = 100000$. The results of this additional study are presented in Figure 4 (b). We can see that they are similar to those obtained previously in Figure 3, which means that our method does not seem to be sensitive to the presence of correlation between the columns of \mathbf{W} .

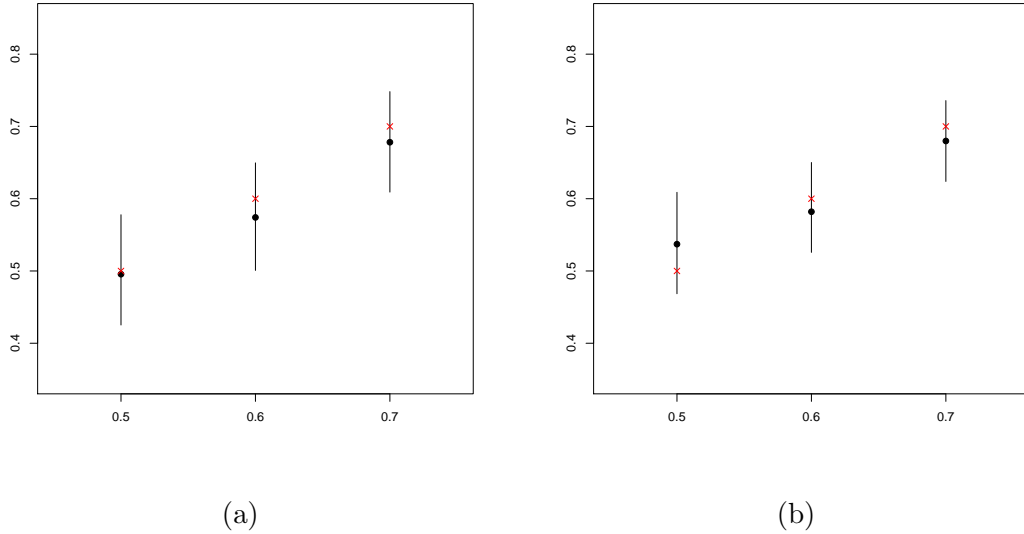


FIGURE 4. Estimated value of the heritability with 95 % confidence intervals. The results are displayed for several values of η^* : 0.5, 0.6 and 0.7. (a) The data sets were generated including fixed effects. (b) The matrix \mathbf{Z} used to generate data sets comes from the IMAGEN data. The black dots correspond to the mean of $\hat{\eta}$ over 10 replications and the crosses are the real value of η^* .

4.2.6. *Computational times.* The implementation that we propose in the R package EstHer is very efficient since it only takes 45 seconds for estimating the heritability and 300 additional seconds to compute the associated 95% confidence interval. These results have been obtained with a computer having the following configuration: RAM 32 GB, CPU 4×2.3 GHz.

4.2.7. *Recovering the support.* When the number of causal SNPs is reasonably small, our variable selection method is efficient to estimate the heritability and we wonder if it is reliable as well to recover the support of the random effects. In Figure 5, we see the proportion of support estimated by our method when there are 100 causal SNPs: our method selects around 130 components. We then focus on the proportion of the real support which has been captured by our method: we see that it may change according to η^* . Indeed, the higher η^* , the higher this proportion. Nevertheless, even in the worst case, that is $\eta^* = 0.5$, Figure 6 shows that even if we keep only 30% of the real non null components, we select the most active ones.

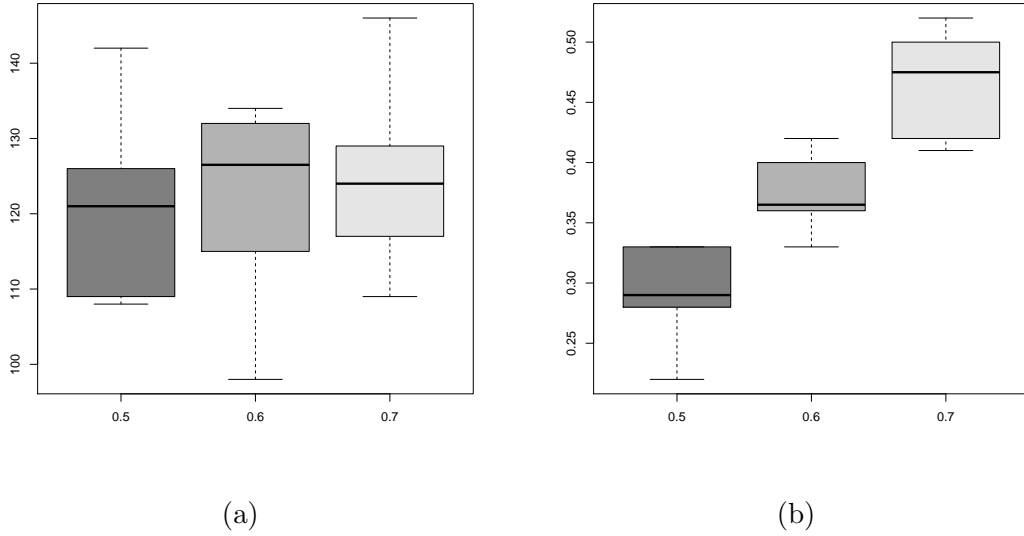


FIGURE 5. (a) Boxplots of the length of the set of selected variables with EstHer for 40 repetitions. The real number of non null components is 100. (b) Boxplots of the proportion of the real non null components captured in the set of selected variables.

The ability of recovering the support in linear models has been studied by [20] in ultra high dimensional cases. The author shows that with a non null probability, the support cannot be estimated under some numerical conditions on the parameters q , N and n (namely if there are considerably more variables N than observations n , and if the number of non null components qN is relatively high). In this simulation study, even when we consider small values of q (for instance $q = 10^{-3}$, that is 100 causal SNPs), we are not far from to the ultra high dimensional framework described in [20], which can explain the difficulties to recover the full support.

4.3. Results when the number of causal SNPs is high. In subsection 4.2 we show the performance of our method in the case where the proportion of causal SNPs q is small, that is around 10^{-3} . In this subsection, we focus on a more polygenic scenario, that includes the cases where thousands of SNPs or ten of thousands of SNPs are causal.

4.3.1. Results when there are SNPs with moderate and weak effects. We first focus on the statistical performance of EstHer when there are a lot of SNPs (1000 or 10000) with small effects (for example, that explain 5% of the phenotypic variations), and a small number

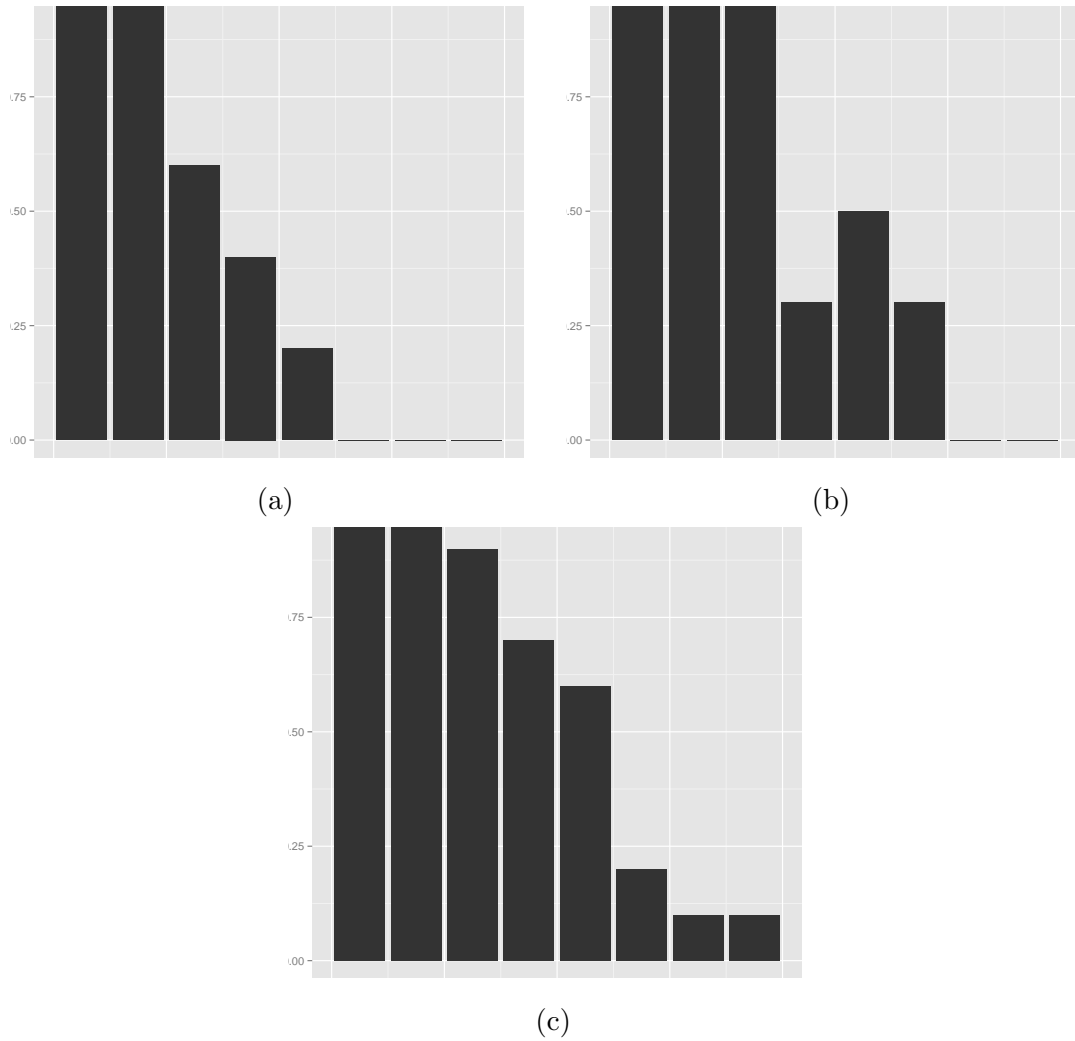


FIGURE 6. Barplots of the proportion of components found by our method as function of the most efficient variables. For example, the first bar is the proportion of the 10 % higher components that we capture with our selection method. The histograms are displayed for several values of η^* : 0.5 (a), 0.6 (b), 0.7 (c).

(around 100) with moderate effects. We can see from Figure 7 that, in this case, EstHer provides unbiased estimations with a small variance.

4.3.2. *Results when all SNPs have moderate effects.* If all causal SNPs have moderate effects and if the number of these causal SNPs is high, namely greater than 1000, EstHer underestimates the heritability. These results are displayed in Figure 8. Moreover, we can see from

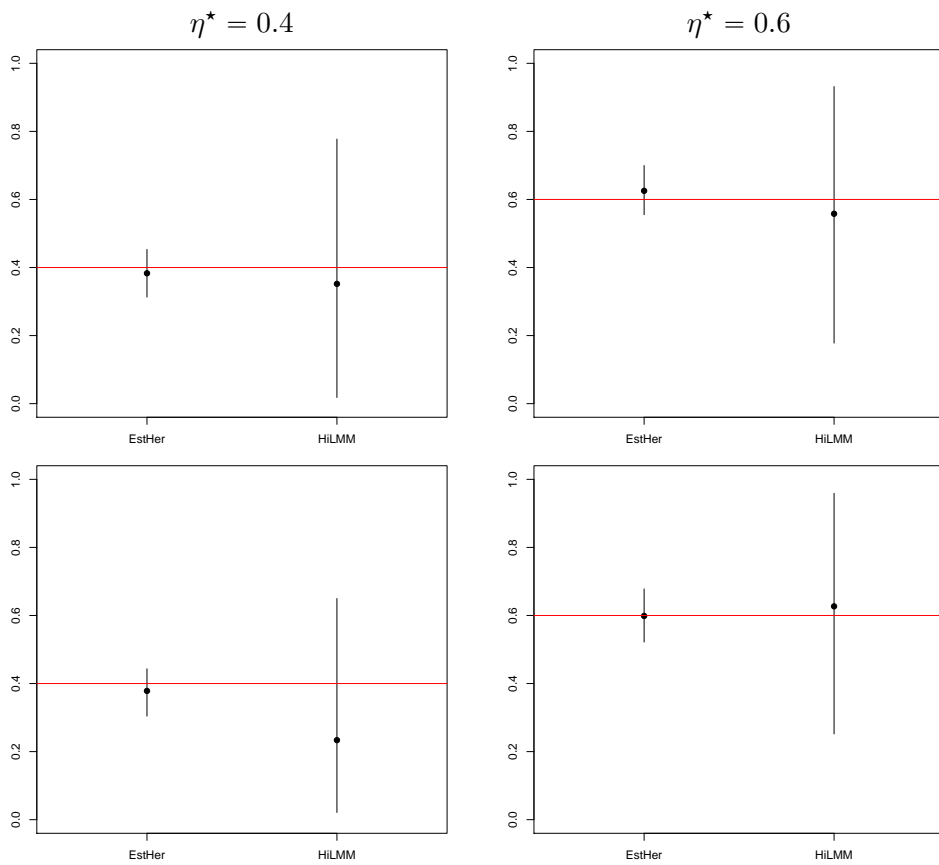


FIGURE 7. Results of HiLMM and EstHer when there are a few causal SNPs with moderate effects and a lot of SNPs with small effects. The proportion of each is 100 out of 1000 (up) and 100 out of 10000 (bottom), with $\eta^* = 0.4$ and 0.6.

Figure 9 that there is no threshold choice that can provide accurate estimations of heritability for all values of η^* .

5. A CRITERION TO DECIDE WHETHER WE SHOULD APPLY ESTHER OR HILMM

On the one hand, we observed that applying HiLMM provides unbiased estimations of the heritability, no matter the number of causal SNPs. However, the main drawback of this estimator is its very large variance. On the other hand, if the number of causal SNPs is not too high, EstHer provides unbiased estimations of the heritability with standard errors substantially smaller than HiLMM. However, if the number of causal SNPs is high, EstHer

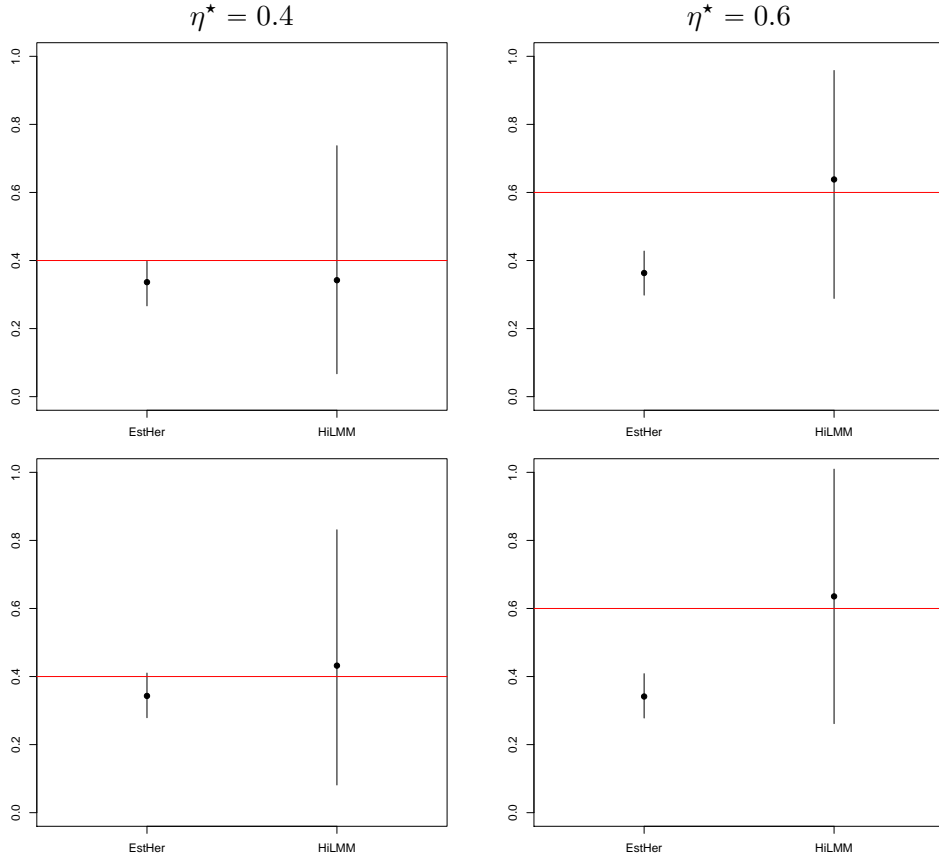


FIGURE 8. Results of HiLMM and EstHer for 1000 (up) and 10000 (bottom) causal SNPs and for $\eta^* = 0.4$ and 0.6 .

underestimates the heritability. These observations are similar to those made by [23], who built an hybrid estimator able to deal with both sparse and non sparse scenario, to which we will compare our approach in Section 6. Therefore, we propose hereafter a rule to decide whether it is better to apply EstHer or HiLMM. We can see from Figure 2 that when there are 100 causal SNPs, there is a large range of threshold values which provide an accurate estimation of η^* , but when there are 1000 or 10000 causal SNPs, see Figure 9), the estimations are very different even for close thresholds. This observation gave us the idea of quantifying the stability of the estimations around the threshold that we determined as the optimal one. More precisely, for each threshold, we have an estimation of heritability with a 95% confidence interval, and we count the number of thresholds for which the confidence intervals overlap. Figure 10 confirms the stability around the best threshold for different values of η^*

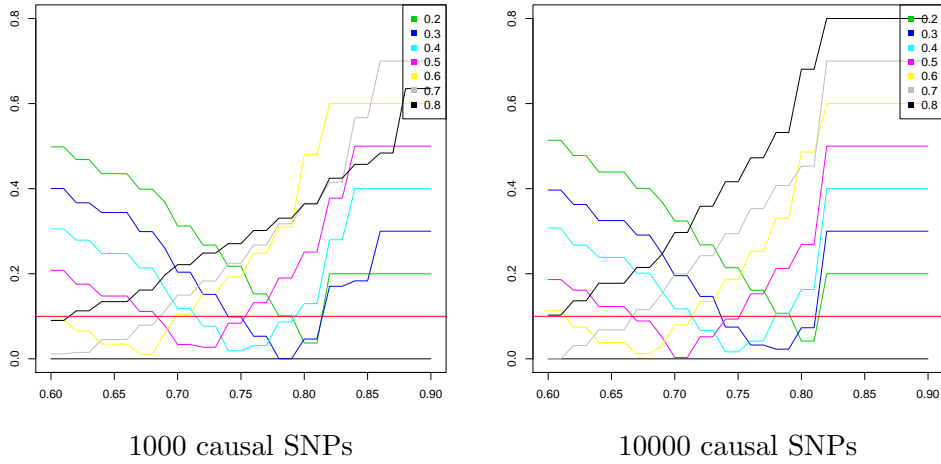


FIGURE 9. Absolute difference $|\eta^* - \hat{\eta}|$ for thresholds from 0.6 to 0.9 and for 1000 (left) and 10000 (right) causal SNPs.

TABLE 3. Mean value of the number of overlapping confidence intervals for 16 thresholds from 0.7 to 0.85.

η^*	100 causal SNPs	1000 causal SNPs	10000 causal SNPs
0.4	11.9	8.1	7.8
0.5	15.3	6.9	7
0.6	16	9.2	7.1

and Table 3 displays the number of overlapping confidence intervals. We empirically determine the following criterion: if the mean number of thresholds is greater than 10 (over 16 tested thresholds), we apply EstHer, if not, we apply HiLMM. The results obtained by using this criterion are displayed in Figure 11.

6. RESULTS AFTER APPLYING THE DECISION CRITERION AND COMPARISON TO OTHER METHODS

6.1. Statistical performances. In this section we show the results obtained after applying the criterion described in Section 5. We compare these results to those obtained using HiLMM, but also with the software GEMMA described in [24]. GEMMA can fit both a non sparse

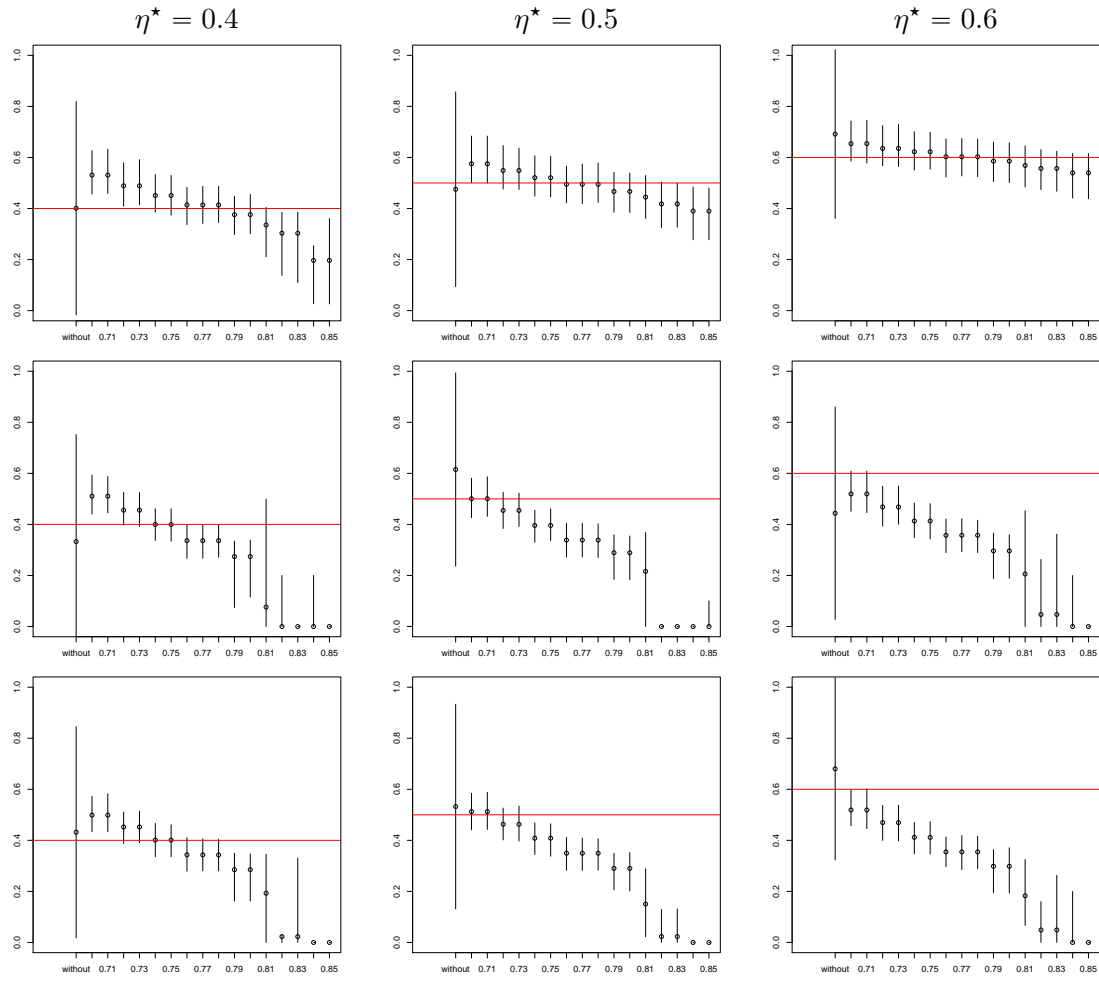


FIGURE 10. Estimation of the heritability with 95% confidence intervals for η^* from 0.4 to 0.6 (from left to right), and from 100, 1000 and 10000 causal SNPs from top to bottom. Each graph shows the heritability estimations with 95% confidence intervals computed with HiLMM (“without”) and for thresholds between 0.7 and 0.85.

linear mixed model (GEMMA-LMM) and a sparse linear mixed model if the BSLMM option is chosen denoted by BSLMM in the sequel. As explained in [23], BSLMM can deal with very sparse and also with very polygenic scenarios.

We can see from the bottom part of Figure 11 that, in very polygenic scenarios ($q = 0.1$, namely 10,000 causal SNPs), all the methods provide similar results: the four estimators are indeed empirically unbiased, but with a very large variance.

In sparse scenarios ($q = 10^{-3}$, namely 100 causal SNPs), we can see from the top part of Figure 11 that EstHer provides better results than HiLMM and GEMMA-LMM which exhibit similar statistical performances. In sparse scenarios, the variance of the BSLMM estimator is larger than the one provided by EstHer and smaller than the one provided by GEMMA-LMM and HiLMM. However, the performances of BSLMM could perhaps be improved by changing the MCMC parameters. Here, for computational time reasons, we used the default parameters that is 100,000 and 1,000,000 for the number of burn-in steps and the number of sampling, respectively.

6.2. Computational times. The computational times in seconds for one estimation of the heritability with BSLMM and the heritability estimation for 16 thresholds as well as the associated confidence intervals with our method EstHer are displayed in Figure 12. We chose this number of thresholds since we applied the criterion defined in Section 5. It should be noticed that the computational times for EstHer could be blackuced by diminishing the number of thresholds. For BSLMM we used the default parameters for the number of burn-in steps and the number of sampling. We can see from this figure that the gap between EstHer and BSLMM is all the more important that N is large. Contrary to our approach, BSLMM seems to be very sensitive in terms of computational time to the value of N .

7. APPLICATIONS TO GENETIC DATA

In this section, we applied our method to the neuroanatomic data coming from the Imagen project. In this data set, $n = 2087$ individuals and $N = 273926$ SNPs. For further details on this data set, we refer the reader to Section 2.

7.1. Calibration of the threshold. We start by finding the threshold which is the most adapted to the Imagen data set. We use the same technique as the one described in Section 4.2.1: for several values of η^* and several thresholds, we display the absolute value of $\eta^* - \hat{\eta}$, see Figure 13. The only difference with Section 4.2.1 is that we generated the observations by using the matrix \mathbf{W} coming from the IMAGEN data set. According to Figure 13, we can find a reliable range of thresholds for estimating the heritability for all η^* from 0.4 to 0.7 when

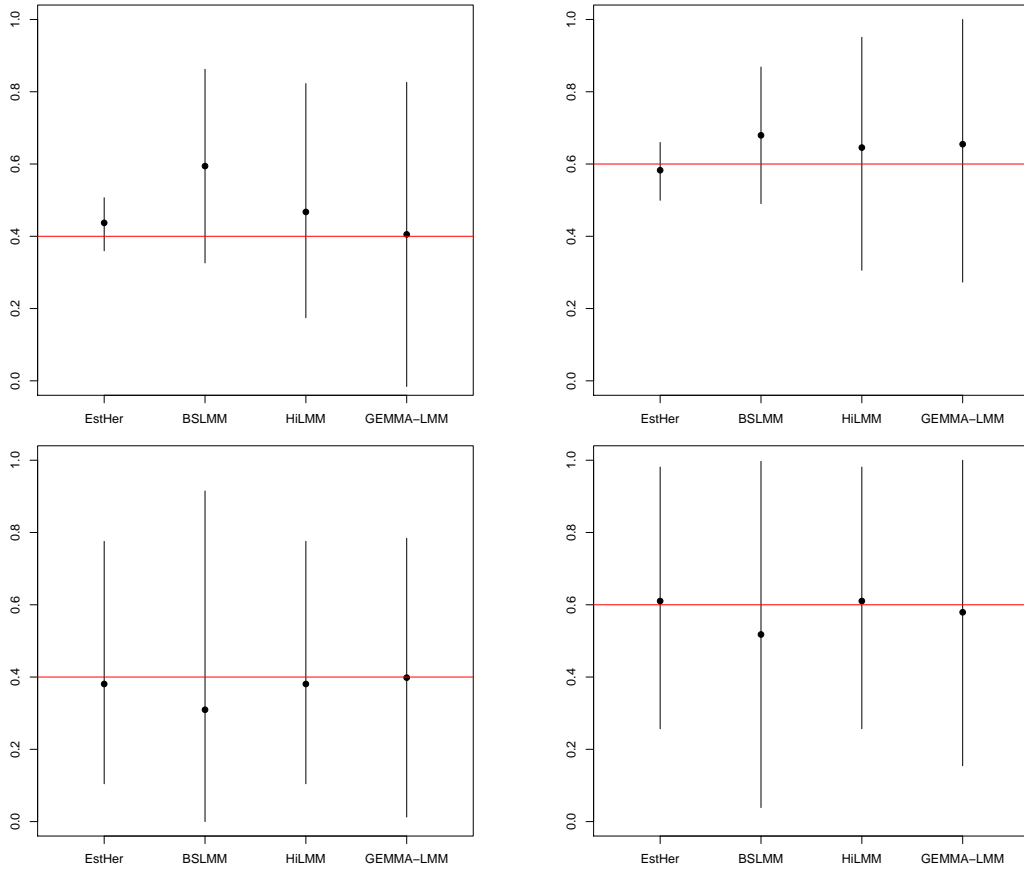


FIGURE 11. Estimations of $\hat{\eta}$ with 95 % confidence intervals obtained using EstHer, BSLMM, HiLMM and GEMMA-LMM with 100 causal SNPs (top) and 10,000 causal SNPs (bottom). The results are obtained with 10 replications.

the number of causal SNPs is smaller than 100. This optimal threshold is equal to 0.79. We shall use this value in the sequel.

7.2. Application of the decision criterion. Since we determined in the previous section that the optimal threshold is 0.79, we apply EstHer for thresholds around this value, that is from 0.7 to 0.85. We then count the number of overlapping confidence intervals, as explained in Section 5. The results are displayed in Table 4. We observe from this table that the sensitivity to the choice of the threshold varies substantially from one phenotype to another. Hence, we choose to apply our EstHer approach to the most stable phenotypes with respect

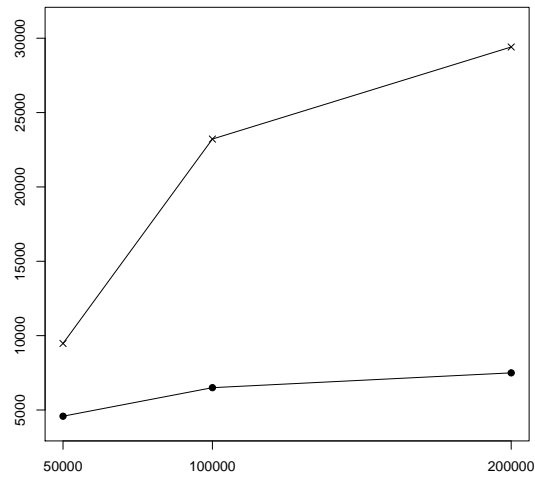


FIGURE 12. Times (in seconds) to compute one heritability estimation with BSLMM (crosses) and EstHer (dots) by using 16 thresholds for $n = 2000$ and different values of N from 50,000 to 200,000.

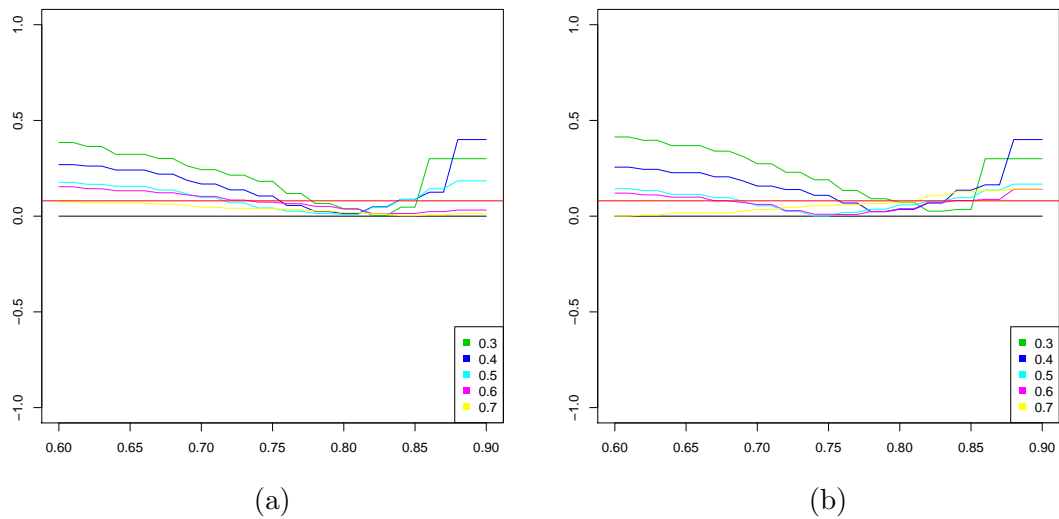


FIGURE 13. Absolute value of the difference between η^* and $\hat{\eta}$ for thresholds from 0.6 to 0.9, and for different values of qN : (a) 50 causal SNPs, (b) 100 causal SNPs. Each difference has been computed as the mean of 10 replications.

to our criterion, namely pa, amy and acc. For the other phenotypes we recommend to apply HiLMM or another similar approach such as GCTA or GEMMA-LMM.

TABLE 4. Mean value of the number of overlapping confidence intervals for 16 thresholds from 0.7 to 0.85.

Phenotype	Number of thresholds
Bv	7.19
Hip	7.5
Icv	7.37
Acc	9.94
Amy	9.88
Th	7.5
Ca	7.13
Pu	7.13
Pa	10.75

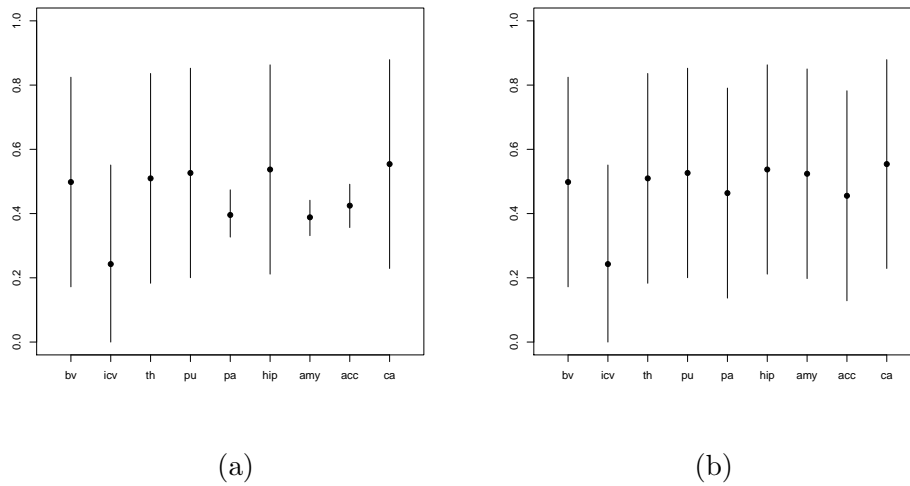


FIGURE 14. (a) Heritability estimations of bv, icv, th, pu, pa, hip, amy, acc, and ca with 95% confidence intervals obtained using EstHer or HiLMM according to the outcome of our decision criterion. (b) Heritability estimations of bv, icv, th, pu, pa, hip, amy, acc and ca with 95% confidence intervals obtained using HiLMM.

7.3. Results. Figure 14 (a) shows the heritability estimation with 95 % confidence intervals for all phenotypes, using either EstHer or HiLMM according to the outcome of our decision criterion. Figure 14 (b) shows the results obtained by using HiLMM, namely without any variable selection step. We compare our results with the ones obtained by [19] who estimated the heritability of the same phenotypes by using the software GCTA. On the one hand, we can see from Figure 14 that in the cases where EstHer is used the confidence intervals given by our methodology are substantially smaller and included in those provided by either HiLMM or [19]. On the other hand, when HiLMM is used our results are on a par with those obtained by [19]. Moreover, our approach provides a list of SNPs which may contribute to the variations of a given phenotype and which could be further analyzed from a biological point of view in order to identify new biological pathways.

8. CONCLUSION

We propose in this paper a practical method to estimate the heritability in sparse linear mixed models using variable selection tools, as well as confidence interval obtained thanks to a non parametric bootstrap approach. Our approach is implemented in the R package EstHer which is available from the Comprehensive R Archive Network (CRAN) and from the web page of the first author. In the course of this study, we showed that our approach has two main features which makes it very attractive. Firstly, it is very efficient from a statistical point of view since it provides confidence intervals considerably smaller than those obtained with methods without variable selection. Secondly, its very low computational burden makes its use feasible on very large data sets coming from quantitative genetics.

Moreover, we observed that the statistical performance of the EstHer approach are all the more impressive that the level of sparsity is high that is when q is small. For this reason, we also proposed an empirical criterion which allows the user to decide whether it is better to apply an approach that takes into account the sparsity and starts with a variable selection stage, namely EstHer, or an approach which ignores the potential sparsity in the observations, namely HiLMM.

ACKNOWLEDGMENTS

The authors would like to thank Nicolai Meinshausen and Nicolas Verzelen for fruitful discussions and the IMAGEN consortium for providing the data.

REFERENCES

- [1] D. G. Amaral, C. M. Schumann, and C. W. Nordahl. Neuroanatomy of autism. *Trends in Neurosciences*, 31(3):137 – 145, 2008.
- [2] A. Beinrucker, U. Dogan, and G. Blanchard. Extensions of Stability Selection using subsamples of observations and covariates, 2014. arXiv:1407.4916v1.
- [3] H. D. Bondell, A. Krishna, and S. K. Ghosh. Joint variable selection for fixed and random effects in linear mixed-effects models. *Biometrics*, 66(4):1069–1077, 2010.
- [4] A. Bonnet, E. Gassiat, and C. Levy-Leduc. Heritability estimation in high-dimensional sparse linear mixed models. *Electronic Journal of Statistics*, 9(2):2099–2129, 2015.
- [5] J. Fan and J. Lv. Sure independence screening for ultrahigh dimensional feature space. *Journal of the Royal Statistical Society: Series B (Statistical Methodology)*, 70(5):849–911, 2008.
- [6] Y. Fan and R. Li. Variable selection in mixed effects models. *Annals of Statistics*, 40(4):2043–2068, 2012.
- [7] Y. Guan and M. Stephens. Bayesian variable selection regression for genome-wide association studies and other large-scale problems. *The Annals of Applied Statistics*, 5(3):1780–1815, 09 2011.
- [8] P. Ji and J. Jin. UPS delivers optimal phase diagram in high-dimensional variable selection. *Annals of Statistics*, 40(1):73–103, 2012.
- [9] B. Maher. Personal genomes: The case of the missing heritability. *Nature*, 456(7218):18–21, 2008.
- [10] T. A. Manolio, F. S. Collins, N. J. Cox, D. B. Goldstein, L. A. Hindorff, D. J. Hunter, M. I. McCarthy, E. M. Ramos, L. R. Cardon, A. Chakravarti, J. H. Cho, A. E. Guttmacher, A. Kong, L. Kruglyak, E. Mardis, C. N. Rotimi, M. Slatkin, D. Valle, A. S. Whittemore, M. Boehnke, A. G. Clark, E. E. Eichler, G. Gibson, J. L. Haines, T. F. C. Mackay, S. A. McCarroll, and P. M. Visscher. Finding the missing heritability of complex diseases. *Nature*, 461(7265):747–753, 2009.
- [11] N. Meinshausen and P. Bühlmann. Stability selection. *Journal of the Royal Statistical Society: Series B (Statistical Methodology)*, 72(4):417–473, 2010.
- [12] N. Meinshausen and P. Buhlmann. Stability selection. *Journal of the Royal Statistical Society*, 72(4):417–473, 2010.
- [13] H. Patterson and R. Thompson. Recovery of inter-block information when block sizes are unequal. *Biometrika*, 58:545–554, 1971.
- [14] M. Pirinen, P. Donnelly, and C. C. A. Spencer. Efficient computation with a linear mixed model on large-scale data sets with applications to genetic studies. *The Annals of Applied Statistics*, 7(1):369–390, 2013.
- [15] S. Searle, G. Casella, and C. McCulloch. *Variance Components*. Wiley Series in Probability and Statistics. Wiley, 1992.
- [16] R. G. Steen, C. Mull, R. McClure, R. M. Hamer, and J. A. Lieberman. Brain volume in first-episode schizophrenia. *The British Journal of Psychiatry*, 188(6):510–518, 2006.

- [17] J. L. Stein, S. E. Medland, A. A. Vasquez, D. P. Hibar, R. E. Senstad, A. M. Winkler, R. Toro, K. Appel, R. Bartecek, O. Bergmann, M. Bernard, A. A. Brown, D. M. Cannon, M. M. Chakravarty, A. Christoforou, M. Domin, O. Grimm, M. Hollinshead, A. J. Holmes, G. Homuth, J.-J. Hottenga, C. Langan, L. M. Lopez, N. K. Hansell, K. S. Hwang, S. Kim, G. Laje, P. H. Lee, X. Liu, E. Loth, A. Lourdasamy, M. Mattingsdal, S. Mohnke, S. M. Maniega, K. Nho, A. C. Nugent, C. O'Brien, M. Pappmeyer, B. Putz, A. Ramasamy, J. Rasmussen, M. Rijpkema, S. L. Risacher, J. C. Roddey, E. J. Rose, M. Ryten, L. Shen, E. Sprooten, E. Strengman, A. Teumer, D. Trabzuni, J. Turner, K. van Eijk, T. G. M. van Erp, M.-J. van Tol, K. Wittfeld, C. Wolf, S. Woudstra, A. Aleman, S. Alhusaini, L. Almasy, E. B. Binder, D. G. Brohawn, R. M. Cantor, M. A. Carless, A. Corvin, M. Czisch, J. E. Curran, G. Davies, M. A. A. de Almeida, N. Delanty, C. Depondt, R. Duggirala, T. D. Dyer, S. Erk, J. Fagerness, P. T. Fox, N. B. Freimer, M. Gill, H. H. H. Goring, D. J. Hagler, D. Hoehn, F. Holsboer, M. Hoogman, N. Hosten, N. Jahanshad, M. P. Johnson, D. Kasperaviciute, J. W. Kent, P. Kochunov, J. L. Lancaster, S. M. Lawrie, D. C. Liewald, R. Mandl, M. Matarin, M. Mattheisen, E. Meisenzahl, I. Melle, E. K. Moses, T. W. Muhleisen, M. Nauck, M. M. Nothen, R. L. Olvera, M. Pandolfo, G. B. Pike, R. Puls, I. Reinvang, M. E. Renteria, M. Rietschel, J. L. Roffman, N. A. Royle, D. Rujescu, J. Savitz, H. G. Schnack, K. Schnell, N. Seiferth, C. Smith, V. M. Steen, M. C. Valdes Hernandez, M. Van den Heuvel, N. J. van der Wee, N. E. M. Van Haren, J. A. Veltman, H. Volzke, R. Walker, L. T. Westlye, C. D. Whelan, I. Agartz, D. I. Boomsma, G. L. Cavalleri, A. M. Dale, S. Djurovic, W. C. Drevets, P. Hagoort, J. Hall, A. Heinz, C. R. Jack, T. M. Foroud, S. Le Hellard, F. Macciardi, G. W. Montgomery, J. B. Poline, D. J. Porteous, S. M. Sisodiya, J. M. Starr, J. Sussmann, A. W. Toga, D. J. Veltman, H. Walter, M. W. Weiner, J. C. Bis, M. A. Ikram, A. V. Smith, V. Gudnason, C. Tzourio, M. W. Vernooij, L. J. Launer, C. DeCarli, and S. Seshadri. Identification of common variants associated with human hippocampal and intracranial volumes. *Nat Genet*, 44(5):552–561, 2012.
- [18] R. Tibshirani. Regression shrinkage and selection via the lasso. *Journal of the Royal Statistical Society, Series B*, 58(1):267–288, 1996.
- [19] R. Toro, J.-B. Poline, G. Huguet, E. Loth, V. Frouin, T. Banaschewski, G. J. Barker, A. Bokde, C. Büchel, F. Carvalho, P. Conrod, M. Fauth-Bühler, H. Flor, J. Gallinat, H. Garavan, P. Gowloan, A. Heinz, B. Ittermann, C. Lawrence, H. Lemaître, K. Mann, F. Nees, T. Paus, Z. Pausova, M. Rietschel, T. Robbins, M. Smolka, A. Ströhle, G. Schumann, and T. Bourgeron. Genomic architecture of human neuroanatomical diversity. *Molecular Psychiatry*, 20(8):1011–1016, 2015.
- [20] N. Verzelen. Minimax risks for sparse regressions: Ultra-high dimensional phenomena. *Electronic Journal of Statistics*, 6:38–90, 2012.
- [21] J. Yang, B. Benyamin, B. P. McEvoy, S. Gordon, A. K. Henders, D. R. Nyholt, P. A. Madden, A. C. Heath, N. G. Martin, G. W. Montgomery, M. E. Goddard, and P. M. Visscher. Common snps explain a large proportion of the heritability for human height. *Nature Genetics*, 42(7):565–569, 2010.
- [22] J. Yang, S. H. Lee, M. E. Goddard, and P. M. Visscher. GCTA: A tool for genome-wide complex trait analysis. *The American Journal of Human Genetics*, 88(1):76 – 82, 2011.

- [23] X. Zhou, P. Carbonetto, and M. Stephens. Polygenic modeling with bayesian sparse linear mixed models. *PLoS genetics*, 9(2):e1003264, 2013.
- [24] X. Zhou and M. Stephens. Genome-wide efficient mixed model analysis for association studies. *Nature Genetics*, 44:821–824, 2012.

LABORATOIRE DE MATHÉMATIQUES D'ORSAY, UNIV. PARIS-SUD, CNRS, UNIVERSITÉ PARIS-SACLAY,
91405 ORSAY, FRANCE

E-mail address: `elisabeth.gassiat@math.u-psud.fr`

AGROPARISTECH/UMR INRA MIA 518

E-mail address: `celine.levy-leduc@agroparistech.fr`, `anna.bonnet@agroparistech.fr`

HUMAN GENETICS AND COGNITIVE FUNCTIONS, INSTITUT PASTEUR, PARIS, FRANCE

E-mail address: `rto@pasteur.fr`, `thomasb@pasteur.fr`